

# Kinetics of hydrolysis of chitin/chitosan oligomers in concentrated hydrochloric acid

Aslak Einbu, Hans Grasdalen and Kjell M. Vårum\*

*Norwegian Biopolymer Laboratory (NOBIPOL), Department of Biotechnology,  
Norwegian University of Science and Technology, 7491 Trondheim, Norway*

Received 21 December 2006; received in revised form 9 February 2007; accepted 19 February 2007

Available online 24 February 2007

**Abstract**—The kinetics of hydrolysis in concentrated hydrochloric acid (12.07 M) of the fully N-acetylated chitin tetramer (GlcNAc<sub>4</sub>) and the fully N-deacetylated chitosan tetramer (GlcN<sub>4</sub>) were followed by determining the amounts of the lower DP oligomers as a function of time. A theoretical model was developed to simulate the kinetics of hydrolysis of the three different glycosidic linkages in the tetramers. The model uses two different rate constants for the hydrolysis of the glycosidic bonds in the oligomers, assuming that the glycosidic bond next to one of the end residues are hydrolysed faster than the two other glycosidic linkages. The two rate constants were estimated by fitting model data to experimental results. The results show that the hydrolysis of the tetramers is a nonrandom process as the glycosidic bonds next to one of the end residues are hydrolysed 2.5 and 2.0 times faster as compared to the other glycosidic linkages in the fully N-acetylated and fully N-deacetylated tetramer, respectively. From previous results on other oligomers and the reaction mechanism, it is likely that the glycosidic bond that is hydrolysed fastest is the one next to the nonreducing end. The absolute values for the rate constants for the hydrolysis of the glycosidic linkages in GlcNAc<sub>4</sub> were found to be 50 times higher as compared to the glycosidic linkages in GlcN<sub>4</sub>, due to the catalytic role of the N-acetyl group and the presence of the positively charged amino-group on the N-deacetylated sugar residue.

© 2007 Elsevier Ltd. All rights reserved.

**Keywords:** Oligomer; Acid-catalysed hydrolysis; Theoretical model; Reaction rate constants

## 1. Introduction

Acid-catalysed hydrolysis of glycosidic linkages can occur with widely varying reaction rates, depending on, for example, ring size, configuration, conformation and structure of the glycon. Differences in reaction rates can be utilised for characterisation of polysaccharides after purification and subsequent structural characterisation of the oligosaccharides from acid-catalysed hydrolysis.<sup>1</sup> One example of a very large difference in the relative rates of acid-catalysed hydrolysis of glycosidic linkages in the same polysaccharide is from chitosans, a family of polysaccharides composed of (1→4)-linked 2-amino-2-deoxy-β-D-glucopyranose units

(glucosamine) that can be N-acetylated to varying extents. The glycosidic linkage following an N-acetylated unit has been found to be hydrolysed at conditions favouring acid-catalysed hydrolysis three orders of magnitude faster as compared to the glycosidic linkage following a N-deacetylated unit.<sup>2</sup> This can be explained by two main factors, that is, a catalytic role of the N-acetyl group at carbon 2 which stabilises the oxocarbenium ion transition state resulting in an enhanced rate of cleavage of the glycosidic linkage following the N-acetylated residue,<sup>3</sup> and the presence of a positively charged amino-group at carbon 2 in a glucosamine residue that would shield the glycosidic oxygen from protonation and thereby result in a decreased rate of cleavage of the glycosidic linkage following a glucosamine residue.<sup>4</sup>

A complicating factor when studying acid-catalysed hydrolysis of chitin oligomers is the concomitant acid-catalysed N-deacetylation reaction. However, in

\* Corresponding author. Tel.: +47 73593324; fax: +47 73591283;  
e-mail: [kvaarum@nt.ntnu.no](mailto:kvaarum@nt.ntnu.no)

concentrated hydrochloric acid (12.07 M), the rate of acid-catalysed cleavage of the glycosidic linkage was found to be much higher than the N-deacetylation reaction.<sup>2,5,6</sup> Thus, at this high acid concentration a study of the acid-catalysed cleavage of the glycosidic linkages without concomitant N-deacetylation should be possible. The acid-catalysed hydrolysis of starch, cellulose and chitin has been reported to be a nonrandom depolymerisation reaction.<sup>2,7,8</sup> When the calculated amounts of D-glucose and oligosaccharides liberated by the hydrolysis of a given weight of starch or cellulose are compared with the actual amounts formed, it was found that there are more products of low degree of polymerisation and fewer intermediate-sized products than would be expected from a completely random hydrolysis, for any degree or time of hydrolysis.<sup>8,9</sup> Thus, it appears that acid-catalysed hydrolysis does not occur by random scission. However, a complicating factor when studying acid-catalysed depolymerisation of polysaccharides such as cellulose and chitin is their insolubility in aqueous solvents.<sup>5</sup>

The most accepted reaction mechanism for the acid-catalysed hydrolysis of a glycosidic linkage is illustrated in Chart 1.

The mechanism involves protonation of the glycosidic oxygen atom to form the conjugate acid, followed by heterolysis of the exocyclic O-5 to C-1 bond to give a cyclic carbonium–oxonium ion which most probably exists in the half-chair conformation having C-2, C-1, O-5 and C-5 in a plane. Reaction with water then gives the protonated reducing sugar, and from it, the reducing sugar is formed. The nonrandom acid-catalysed hydrolysis of polysaccharides can be explained by this reaction mechanism, as the glycosidic linkage at the nonreducing end is hydrolysed more rapidly than the other glycosidic linkages in the chain. This conclusion was reached from the fact that hydrolysis of an internal linkage would involve, in the formation of the carbonium–oxonium ion, reorientation of an entire chain; that is, hydrolysis would be diminished by the introduction of a large bulky group, in a manner similar to what has been

found for the introduction of various sized groups at C-5.<sup>1</sup>

Acid-catalysed hydrolysis of model oligosaccharides of defined composition and chain length has certain advantages compared to polysaccharides, such as full water-solubility and fully defined composition and chain length, and such studies have been mainly focused on comparing the rates of terminal glycosidic linkages in relation to internal linkages. Jones et al.<sup>10</sup> concluded that the bond of one of the end residues of isomaltotriose is hydrolysed 1.7 times faster as compared to the reducing end. Weintraub and French<sup>11</sup> showed experimentally that the glycosidic linkage next to the nonreducing end of starch chains was hydrolysed the fastest by acid. Furthermore, the rate constants for acid-catalysed hydrolysis of the nonreducing end glycosidic linkages of maltotriose and maltohexose were found to be 1.8 times higher as compared to the other glycosidic linkages.<sup>12</sup> Feather and Harris studied the kinetics of the hydrolysis of cellotriose, and compared their experimental data with model data and found that the rate of hydrolysis of the nonreducing end glycosidic linkage was 1.5 times higher compared to the reducing end glycosidic linkage.<sup>13</sup> However, to the best of our knowledge, modelling of the hydrolysis of the glycosidic linkages of a tetramer has not been published. We now report a study on the kinetics of hydrolysis of the three glycosidic linkages of the fully N-acetylated chitin tetramer and the fully N-deacetylated chitosan tetramer in concentrated HCl. The formation of the different oligomers as a function of time were followed quantitatively, and compared and optimised to model data on the formation of oligomers obtained by assuming a different rate for the hydrolysis of the bond of the nonreducing end residue as compared to the other two glycosidic linkages, and very good correlations were obtained when rates of hydrolysis of the bond of one of the end residues were 2.5 and 2.0 times higher as compared to the other two glycosidic linkages for the fully N-acetylated and fully N-deacetylated tetramers, respectively.

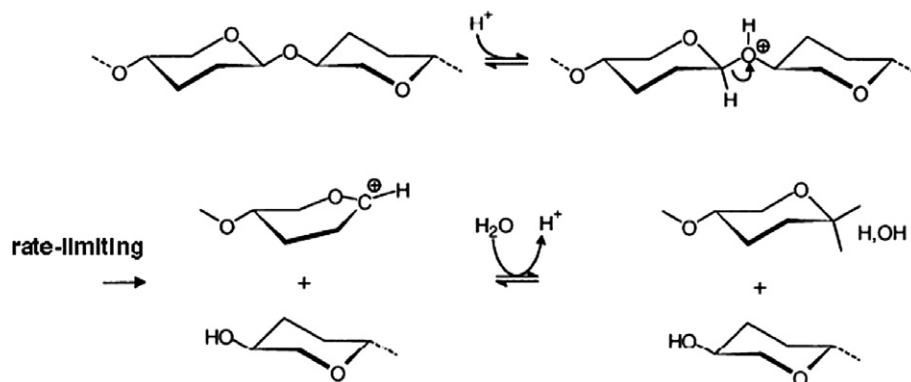


**Chart 1.** Schematic illustration of the proposed reaction mechanism for the acid-catalysed hydrolysis of the glycosidic linkage.

## 2. Experimental

### 2.1. Hydrolysis of chitin/chitosan tetramer in concentrated HCl

To samples of GlcNAc<sub>4</sub> and GlcN<sub>4</sub> (2 mg) (Seikagaku, Japan) were added 100  $\mu$ L concentrated hydrochloric acid (12.07 M) and the samples were incubated at 40 °C. The reaction was stopped by cooling the solution on dry ice and then adjusting the pH to 4.5 with NaOH to prevent heating of the sample upon dilution. Prior to the reaction, the HCl was saturated with nitrogen gas to remove oxygen in order to prevent oxidation reactions. The reaction mixture was kept in reaction tubes which were sealed during reaction.

### 2.2. Size-exclusion chromatography (SEC) of reaction products

The oligomers from the neutralised reaction mixtures were separated on three Superdex™30 columns connected in series as previously described.<sup>14</sup> (Amersham Pharmacia Biotech, overall dimensions 2.6  $\times$  180 cm). The columns were eluted with 0.15 M ammonium acetate, pH 4.5 at a flow rate of 0.8 mL/min. The effluent was monitored with an online refractive index (RI) detector (Shimadzu RID 6A, Shimadzu Schweiz GmbH, Reinach, Switzerland), coupled to a data logger. Sørboten et al.<sup>14</sup> investigated the relationship between detector response and the mass of injected oligomer when using fully acetylated and fully N-deacetylated dimer, tetramer and hexamer. Within the accuracy of the area determination, there was a linear relationship between peak areas and the amount (mass) of injected oligomer, irrespective of DP and degree of acetylation. On the basis of this, the molar fractions of the different oligomers can be calculated from the integrals of the chromatograms from SEC.

### 2.3. Fitting of the mathematical model for hydrolysis to experimental data

The differential equations in Section 3 were solved by programming symbolic algebra in Maple 10. Fitting of the mathematical model to the experimental data was done in EXCEL, using an iteration procedure to minimise the sum of the root mean square deviations for experimental and theoretical molar fractions of all oligomers.

## 3. Theory

### 3.1. Theoretical model for depolymerisation of a tetramer

A model was developed in order to evaluate the hydrolysis of a tetramer compound.

Our model for hydrolysis of a tetramer is based on the hypothesis that the glycosidic bond next to one of the end residues of an oligosaccharide undergoes hydrolysis more rapidly than the other bonds. Based on this assumption, the model applies two different rate constants: rate constant  $k_1$  refers to the hydrolysis of the glycosidic linkage next to one of the end residues of the oligomer while the rate constant  $k_2$  refers to the hydrolysis of the other glycosidic linkages.

Chart 2 shows a model for the cleavage and formation of the different oligomers starting from the tetramer, and forms the basis for the four differential equations describing the formation and cleavage of the oligomers during hydrolysis with rate constants  $k_1$  and  $k_2$ . In Chart 2 it has been assumed that the rate constant for the hydrolysis of the glycosidic linkage next to the *nonreducing end* ( $k_1$ ) is hydrolysed faster than the other glycosidic linkages.

The change in the molar concentrations of the different oligomers in the reaction mixture during hydrolysis can be expressed by differential equations derived from the cleavage and formation of the different oligomers as seen schematically in Chart 2.

The tetramer can either be split into two dimers or one trimer and one monomer (Chart 2). Eq. 1 expresses the decay in the molar concentration of tetramer,  $[A_4]$ , as a function of  $[A_4]$ , and the rate constants  $k_1$  and  $k_2$

$$\frac{d}{dt}[A_4] = -[A_4] \cdot (k_1 + 2k_2) \quad (1)$$

Solving Eq. 1 with initial value of  $[A_4(0)] = 1$ , gives Eq. 2 expressing  $[A_4]$  as a function of  $k_1$ ,  $k_2$  and time,  $t$

$$[A_4] = e^{-(k_1 + 2k_2)t} \quad (2)$$

The trimer can only be formed from cleavage of the tetramer, while it can be cleaved to form a dimer and a

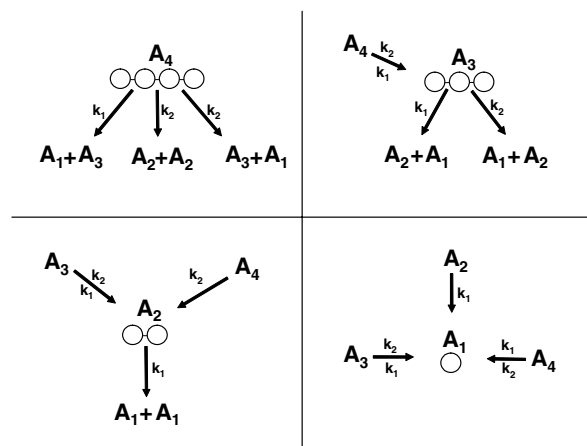


**Chart 2.** Cleavage and formation of the different oligomers starting from the tetramer,  $A_4$  (top left), trimer,  $A_3$  (top right), dimer,  $A_2$  (down left) and monomer,  $A_1$  (down right). The hydrolysis of the glycosidic bonds are described by the rate constants  $k_1$  and  $k_2$ .

monomer by two different rate constants (Chart 2). The change in the molar amount of trimer,  $[A_3]$ , in the reaction mixture is expressed in Eq. 3 as a function of  $[A_4]$  (Eq. 2),  $[A_3]$ , and the rate constants  $k_1$  and  $k_2$ .

$$\frac{d}{dt}[A_3] = [A_4] \cdot (k_1 + k_2) - [A_3] \cdot (k_1 + k_2) \quad (3)$$

The first term of Eq. 3 represents the formation of trimer from tetramer, and the second term represents the degradation of trimer. Solving Eq. 3 with initial conditions  $[A_4(0)] = 1$  and  $[A_3(0)] = 0$  gives Eq. 4 which describes  $[A_3]$  as a function of time and the rate constants  $k_1$  and  $k_2$ .

$$[A_3] = \frac{k_1 + k_2}{k_2} \cdot (e^{-(k_1 + k_2)t} - e^{-(k_1 + 2k_2)t}) \quad (4)$$

Eq. 5 expresses the change in the molar amount of the dimer,  $[A_2]$ , with time.

$$\frac{d}{dt}[A_2] = [A_4] \cdot 2k_2 + [A_3] \cdot (k_1 + k_2) - [A_2] \cdot k_1 \quad (5)$$

The first term represents the formation of dimer from the tetramer, the second term the formation of dimer from the trimer and the last term the degradation of the dimer (Chart 2). Solving Eq. 5 with initial conditions  $[A_4(0)] = 1$ ,  $[A_3(0)] = 0$  and  $[A_2(0)] = 0$  gives Eq. 6 which expresses the  $[A_2]$  as a function of time,  $k_1$  and  $k_2$

$$[A_2] = \left(1 + \frac{(k_1 + k_2)^2}{2k_2^2}\right) \cdot e^{-k_1 t} - \left(\frac{(k_1 + k_2)^2}{k_2^2}\right) \cdot e^{-(k_1 + k_2)t} - \left(1 - \frac{(k_1 + k_2)^2}{2k_2^2}\right) \cdot e^{-(k_1 + 2k_2)t} \quad (6)$$

The increase in the molar amount of monomer,  $[A_1]$ , with time is similarly given by Eq. 7 (see Chart 2)

$$\frac{d}{dt}[A_1] = [A_4] \cdot (k_1 + k_2) + [A_3] \cdot (k_1 + k_2) + [A_2] \cdot 2k_1 \quad (7)$$

The three terms of Eq. 7 represents the formation of monomer from tetramer, trimer and dimer, respectively. Solving Eq. 7 with initial conditions  $[A_4(0)] = 1$ ,  $[A_3(0)] = 0$ ,  $[A_2(0)] = 0$  and  $[A_1(0)] = 0$  gives an expression for  $[A_1]$  as a function of time,  $k_1$  and  $k_2$ .

$$[A_1] = \left(2 + \frac{(k_1 + k_2)^2}{k_2^2}\right) \cdot (1 - e^{-k_1 t}) + \frac{k_1 + k_2}{k_2} \cdot \left(1 - 2\frac{k_1}{k_2}\right) \cdot (1 - e^{-(k_1 + k_2)t}) + \left(\frac{k_1 + k_2}{k_1 + 2k_2} - \frac{(k_1 + k_2)^2}{k_2(k_1 + 2k_2)} - \frac{2k_1}{k_1 + 2k_2}\right) \cdot \left(1 - \frac{(k_1 + k_2)^2}{2k_2^2}\right) \cdot (1 - e^{-(k_1 + 2k_2)t}) \quad (8)$$

Eqs. 2, 4, 6 and 7 are used to determine  $[A_4]$ ,  $[A_3]$ ,  $[A_2]$  and  $[A_1]$ , respectively as a function of time with different values of  $k_1$  and  $k_2$ . Using the equations for the molar concentrations of the four oligomers, the theoretical model was compared with experimental molar fractions and estimates of the rate constants  $k_1$  and  $k_2$  were determined as described in Section 2.3.

## 4. Results and discussion

### 4.1. Hydrolysis of the fully N-acetylated chitin tetramer GlcNAc<sub>4</sub> in concentrated HCl

The size-distribution of the oligomers resulting from acid-catalysed hydrolysis of (GlcNAc)<sub>4</sub> in concentrated HCl at 40 °C was followed by gel filtration chromatography as a function of time (Fig. 1). The chromatograms show well-resolved peaks of each oligomer which could be accurately quantified into molar fractions (see Section 2). The tetramer was almost fully hydrolysed to oligomers of a lower DP within 28 h in concentrated HCl at 40 °C. No detectable concentration of oligomers with DP higher than 4 could be seen in the chromatograms, indicating that transglycosylation reactions were insignificant. When the hydrolysis was performed in nitrogen atmosphere (see Section 2), no development of coloured products could be seen even after 28 h, and proton NMR-spectra showed essentially the resonances of the acetylated monomer (data not shown), indicating that any by-products were only present in very low concentrations.

Due to the previously reported much faster hydrolysis of the glycosidic bond compared to the hydrolysis of the N-acetyl linkage of the chitin oligomers in concentrated hydrochloric acid, insignificant N-deacetylation of the oligomers is expected to take place in the time span of the complete hydrolysis of tetramer into monomer.<sup>5,6</sup> The chromatograms in Figure 1 show no detectable amounts of any partially N-deacetylated oligomers, which would appear as separate peaks eluting just after the fully N-acetylated oligomer of the same DP.<sup>14</sup> Hence, no significant N-deacetylation can be detected even after the longest reaction time displayed in Figure 1 (28 h at 40 °C in concentrated HCl), when the molar fraction of monomer is about 0.90.

### 4.2. Comparison of experimental data and model data

The mathematical model for the hydrolysis of a tetramer (see Section 3) was fitted to the molar fractions determined from the chromatograms in Figure 1 by using an iteration procedure to minimise the sum of all root mean square deviations (RMSD) for experimental and theoretical molar fractions of all oligomers. Molar fractions of the four different oligomers together with the

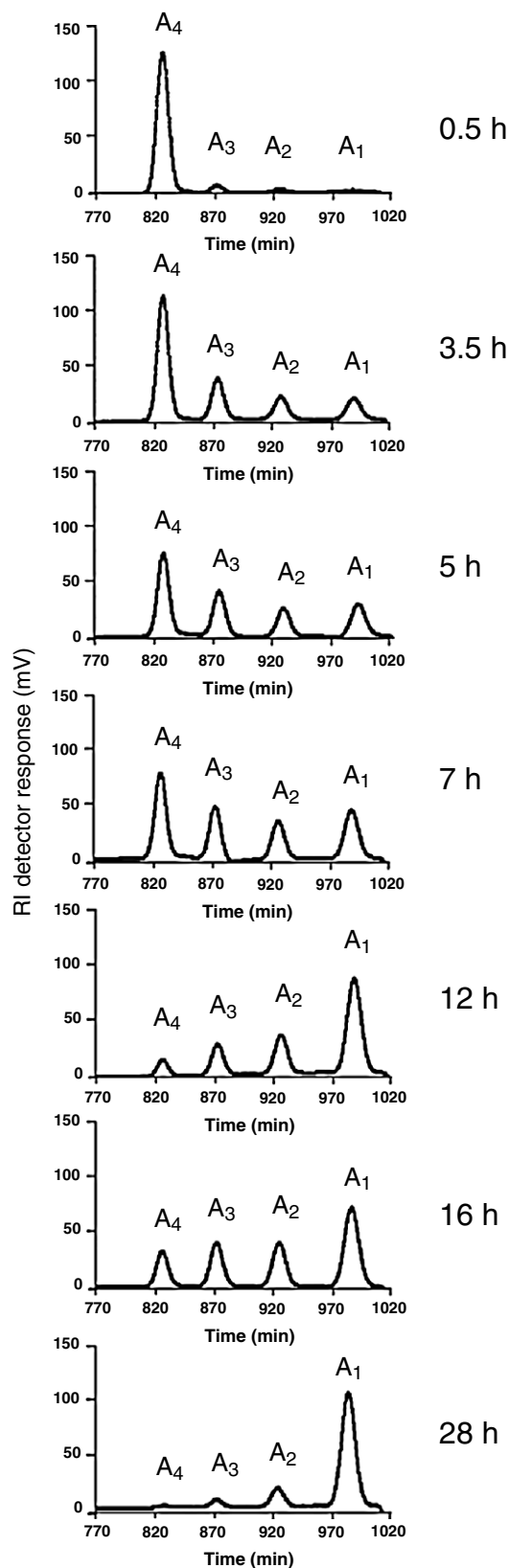


**Figure 1.** Chromatograms showing the size-distribution of oligomers after acid-catalysed hydrolysis of tetra-*N*-acetylchitotetraose with increasing reaction times in concentrated HCl at 40 °C. The gel-filtration chromatograms (Superdex™30) display peaks of the tetramer (A<sub>4</sub>), trimer (A<sub>3</sub>), dimer (A<sub>2</sub>) and monomer (A<sub>1</sub>).

optimised theoretical curves for molar fractions are plotted as a function of time in Figure 2.

The excellent fit between experimental and theoretical data with  $k_1$  2.5 times larger than  $k_2$  indicates that the hydrolysis of the tetramer is a nonrandom process, and that one of the end residues is hydrolysed significantly faster as compared to the other two glycosidic linkages in the tetramer. From previous results on starch and cellulose oligomers,<sup>10–12</sup> and most accepted reaction mechanism (Chart 1), it is likely that the glycosidic bond that is hydrolysed fastest is the one next to the non-reducing end. The difference between the two rate constants is somewhat larger as compared to differences found in, for example, cellotriose.<sup>13</sup>

The robustness of the model with respect to predicting the optimised values of  $k_1$  and  $k_2$  from the experimental data was tested. This is visualised as a contour plot of the sum of all root mean square deviations for experimental and theoretical molar fractions of all oligomers as a function of  $k_1$  and  $k_2$  in Figure 3. From Figure 3, it can be seen that the sum of all root mean square deviations has a global minimum when  $k_1 = 2.5 \times 10^{-5} \text{ s}^{-1}$  and  $k_2 = 1.0 \times 10^{-5} \text{ s}^{-1}$ . Thus, these rate constants represent the optimal fitting of the theoretical data to our experimental results and are the best estimates for the two rate constants in the experiment. The data in Figure 3 clearly visualises that the hydrolysis is a nonrandom process. The diagonal line indicates a random hydrolysis where  $k_1 = k_2$ , whereas the global minimum is located away from the diagonal. The density of the contour intervals around the global minimum also reflect the size of the error estimates for the determined rate constants  $k_1$  and  $k_2$ . From the plot, it can be seen that small changes in the rate constants give significantly higher values for the sum of all root mean square deviations, indicating that the optimised rate constants are robust with respect to predicting rate constants with good accuracy.

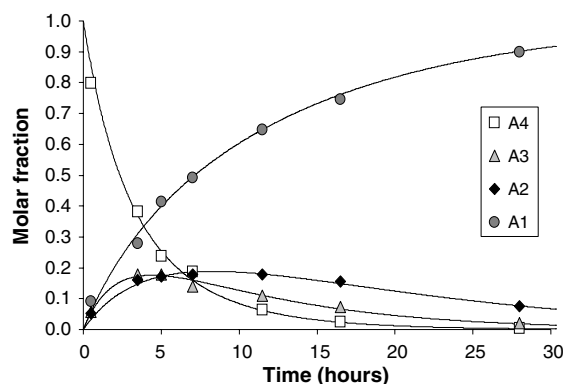


**Figure 2.** Molar fractions of reaction products as a function of time during acid-catalysed hydrolysis of the fully *N*-acetylated chitin tetramer (A<sub>4</sub>) in concentrated hydrochloric acid at 40 °C. Theoretical values for the molar fractions are indicated by continuous lines, with  $k_1 = 2.5 \cdot 10^{-5} \text{ s}^{-1}$  and  $k_2 = 1.0 \cdot 10^{-5} \text{ s}^{-1}$ .



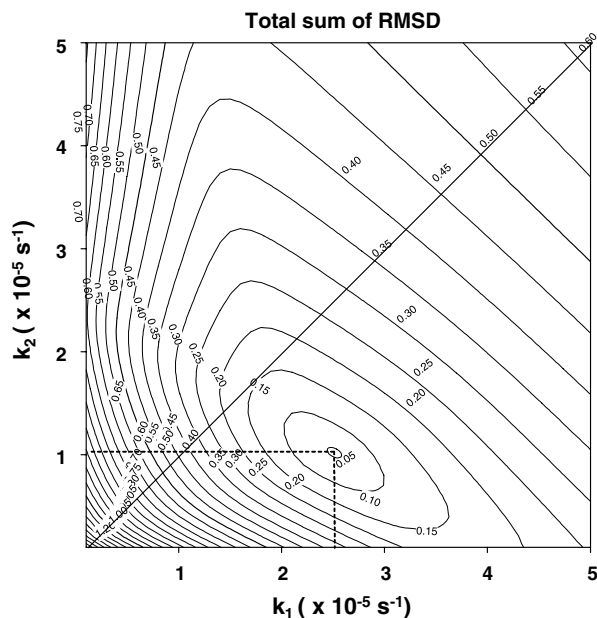


**Figure 3.** Contour plot of the sum of all Root Mean Square Deviations for experimental and theoretical molar fractions of all oligomers as a function of  $k_1$  and  $k_2$ . Contour interval = 0.05.

#### 4.3. Hydrolysis of the fully N-deacetylated chitosan tetramer $\text{GlcN}_4$ in concentrated HCl

The size-distribution of the oligomers resulting from acid-catalysed hydrolysis of the fully N-deacetylated chitosan tetramer in concentrated HCl at 40 °C was also followed by gel filtration chromatography as a function of time (Fig. 4). The chromatograms show well-resolved peaks of oligomers with DP 2–4 which could be quantified into molar fractions (see Section 2).

No evidence of significant transglycosylation reactions (oligomers with DP > 4) or byproducts (coloured products or unidentified resonances in the proton NMR-spectra) when the hydrolysis reaction was performed in nitrogen gas atmosphere. The only exception was the most extensively hydrolysed sample (460 h), which developed a slight yellow-brown colour.

As expected, due to the previously found very much slower rate constant for the acid-catalysed cleavage of the glycosidic linkages followed by a GlcN-unit, the fully N-deacetylated oligomer was hydrolysed much slowly than the acetylated oligomer in concentrated HCl. This can be clearly seen from the very much extended reaction times in order to obtain detectable amounts of the lower oligomers in Figure 4 as compared to Figure 1.

It was not possible to quantify the N-deacetylated monomer, glucosamine, as it was eluting together with the large salt peak (resulting from large amounts of NaCl from neutralisation of the samples of concentrated HCl) in our chromatographic system. Quantifi-

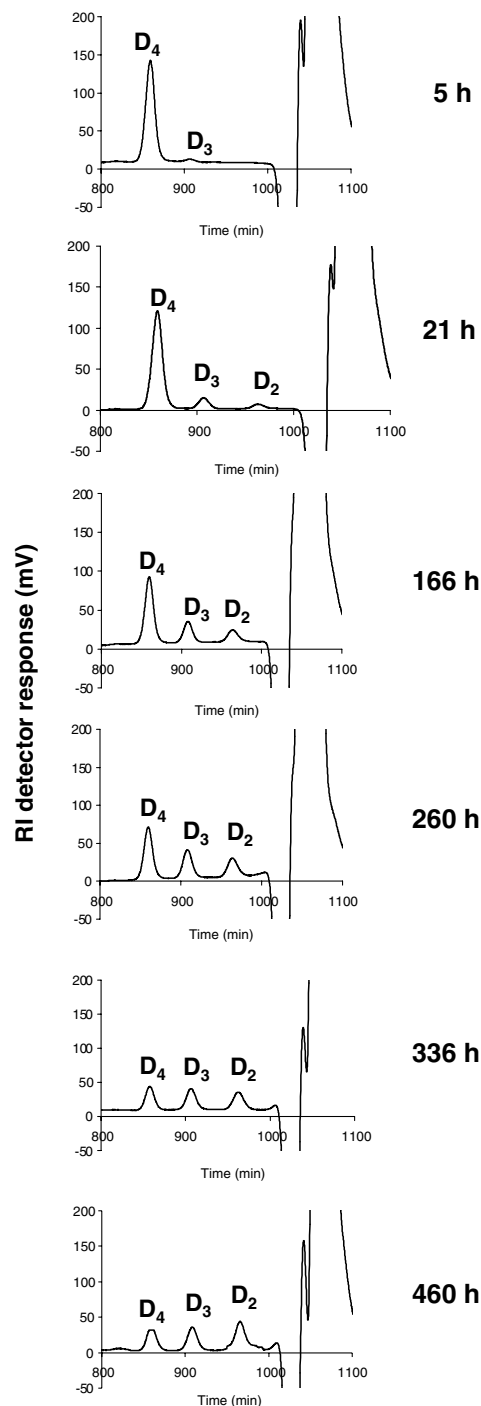


**Figure 4.** Chromatograms showing the size-distribution of oligomers after acid-catalysed hydrolysis of fully N-deacetylated chitosan tetramer with increasing reaction times in concentrated HCl at 40 °C. The gel-filtration chromatograms (Superdex™30) display peaks of the tetramer ( $D_4$ ), trimer ( $D_3$ ) and dimer ( $D_2$ ).

cation of oligomer fractions was therefore restricted to the tetramer, trimer and dimer, which made it impossible to determine the correct molar fractions of the different oligomers. Instead, the sum of relative molar fractions of tetramer, trimer and dimer was set equal

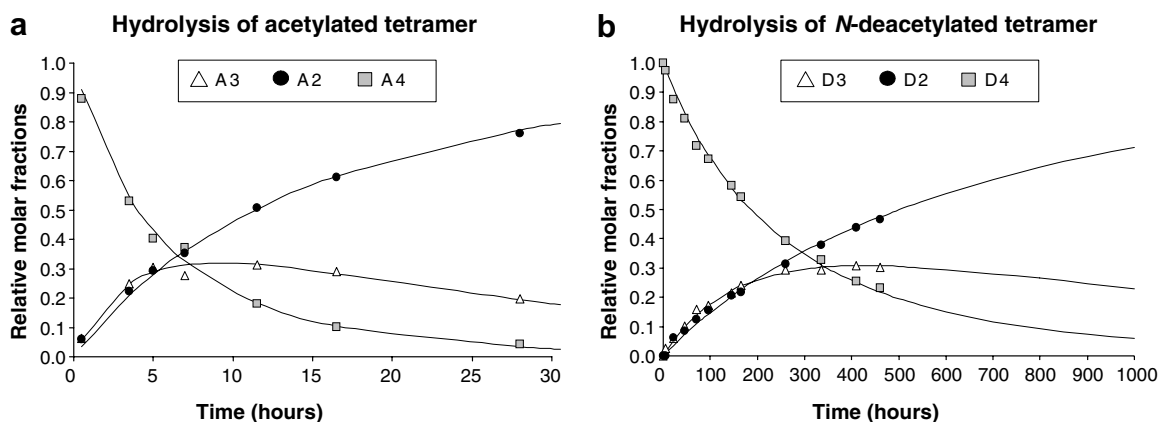


**Figure 5.** Relative molar fractions of tetramer (A4/D4), trimer (A3/D3) and dimer (A2/D2) (as a fraction of the sum of tetramer, trimer and dimer) as a function of time during acid-catalysed hydrolysis in concentrated HCl at 40 °C. Hydrolysis of acetylated tetramer (a) and N-deacetylated tetramer (b). Optimal fitting of the theoretical values for the relative fractions are indicated by continuous lines.

to 1. In order to fit the mathematical model for hydrolysis of chitin tetramer with the experimental results from hydrolysis of the chitosan tetramer, fractions of tetramer, trimer and dimer as a fraction of the sum of all three oligomers were plotted as a function of time in Figure 5b. The results from hydrolysis of GlcNAc<sub>4</sub> were also plotted in the same way in order to directly compare the data from the hydrolysis of GlcN<sub>4</sub> (Fig. 5a).

The continuous lines in Figure 5 show the optimal fitting of the theoretical fractions to the experimental results. The optimal fit was determined when the ratio  $k_1/k_2$  is 2.0 and 2.4 for the hydrolysis of N-deacetylated and acetylated tetramer, respectively. These results indicate that the hydrolysis is a nonrandom process for both tetramers, and the glycosidic linkages next to one of the end residues are hydrolysed faster than the two other glycosidic linkages. As for the results with the chitin oligomers, it is likely to assume that the glycosidic bond that is hydrolysed fastest is the one next to the non-reducing end.

From the continuous lines of the optimal fit in Figure 5b, it seems likely that the model slightly overestimates the amount of tetramer and underestimates the amount of dimer during the initial reaction times. One possible explanation can be a difference in all three reaction rate constants for the cleaving of the three bonds in the tetramer, increasing when going from the reducing end towards the nonreducing end, or vice versa.

#### 4.4. Summary of estimated reaction rate constants

Table 1 summarises values of the reaction rate constants which give the optimal fittings to experimental values in figure as well as the reaction rates determined for the fully N-acetylated chitin tetramer.

The estimated rate constants derived from fitting of our model in Figure 5 are based on data from only three of the four oligomers present, while the estimated rate constants from Figure 2 are based on all four oligomers present during reaction. From the data for hydrolysis of the fully N-acetylated chitin tetramer, it can be seen that the accuracy is slightly better when using all four oligomers (Table 1, last column, row 1 and 2). However, the ratio  $k_1/k_2$  for the hydrolysis of the two different oligomers are the same within the accuracy of the ratios.

The reaction rate constants of the determined for GlcNAc<sub>4</sub> herein are comparable to those determined for GlcNAc<sub>2</sub> previously at the same conditions, taken into account that the previous results were obtained in deuterated hydrochloric acid.<sup>6</sup> The reaction rate constants for the hydrolysis of the glycosidic bonds following an acetylated unit is about 50 times higher as compared to the glycosidic bond following a N-deacetylated unit (Table 1), and can be explained by the catalytic role of the N-acetyl group and the presence of the positively charged amino group in the N-deacetylated unit (see Section 1). This difference between the two constants is at least an order of

**Table 1.** Estimated reaction rate constants,  $k_1$  and  $k_2$ , and the ratio ( $k_1/k_2$ ) for the hydrolysis of GlcNAc<sub>4</sub> and GlcN<sub>4</sub>

	$k_1$ (s <sup>-1</sup> )	$k_2$ (s <sup>-1</sup> )	Ratio ( $k_1/k_2$ )
Hydrolysis of N-acetylated tetramer (estimate from Fig. 2)	$2.5 \pm 0.1 \times 10^{-5}$	$1.0 \pm 0.1 \times 10^{-5}$	$2.5 \pm 0.3$
Hydrolysis of N-acetylated tetramer (estimate from Fig. 5)	$2.4 \pm 0.1 \times 10^{-5}$	$1.0 \pm 0.1 \times 10^{-5}$	$2.4 \pm 0.4$
Hydrolysis of N-deacetylated tetramer (estimate from Fig. 5)	$4.6 \pm 0.2 \times 10^{-7}$	$2.4 \pm 0.2 \times 10^{-7}$	$2.0 \pm 0.3$

magnitude lower as compared to the difference in the rate constants as determined by us previously.<sup>2</sup> However, these rate constants were determined at a different acid concentration and temperature (0.4 M HCl, 60 °C). We speculate that the difference may be explained by a higher relative increase in the rate constant with increasing acid concentration of the N-deacetylated tetramer as compared to the N-acetylated tetramer. However, this could not be verified in a control experiment (data not shown) where the relative rates of the two oligomers were compared at 6 and 12 M HCl, where both oligomers showed the same relative rate increase (~6 times). It is, however, possible that the relative increase in rate constant of the two tetramers could be different at acid concentrations between 0.4 and 6 M, which may explain the discrepancy.

### 5. Conclusions

Reaction rate constants for the hydrolysis of the glycosidic linkages in GlcNAc<sub>4</sub> was found to be 50 times greater as compared to the glycosidic linkages in GlcN<sub>4</sub>. The two tetramers behave similarly in that one of the end glycosidic linkages is hydrolysed 2–2.5 times faster than the other two glycosidic linkages, probably the nonreducing end residue. The model for the depolymerisation of the tetramers described herein can be used to model selectivity in other degradation mechanisms with tetramers as substrates, such as chitinases, chitosanases, amylases and cellulases.

### Acknowledgements

This work was supported by the Norwegian Biopolymer Laboratory (NOBIPOL) and the Norwegian Research Council, Grant 143184/140 ('Calanus'). We thank Olav Smidsrød for valuable discussions.

### References

1. BeMiller, J. N. *Adv. Carbohydr. Chem.* **1967**, 22, 25–108.
2. Vårum, K. M.; Ottøy, M. H.; Smidsrød, O. *Carbohydr. Polym.* **2001**, 46, 89–98.
3. Piszkiwicz, D.; Bruice, T. J. *Am. Chem. Soc.* **1968**, 90, 5844–5848.
4. Moggridge, R. C. G.; Neuberger, A. *J. Am. Chem. Soc.* **1938**, 745, 265–269.
5. Rupley, J. A. *Biochim. Biophys. Acta* **1964**, 83, 245–251.
6. Einbu, A.; Vårum, K. M. *Biomacromol* **2007**, 8, 309–314.
7. Kerr, R. W. In *Chemistry and Industry of Starch*; Academic Press: New York, 1950, Chapter 14.
8. BeMiller, J. N. In *Starch*; Academic Press: New York, 1965; pp 495–499.
9. Purves, C. B. In *Cellulose and Cellulose Derivatives*; Interscience: New York, 1954.
10. Jones, R. W.; Dimler, R. J.; Rist, C. E. *J. Am. Chem. Soc.* **1955**, 77, 1659–1663.
11. Weintraub, M. S.; French, D. *Carbohydr. Res.* **1970**, 15, 241–250.
12. Weintraub, M. S.; French, D. *Carbohydr. Res.* **1970**, 15, 251–262.
13. Feather, M. S.; Harris, J. F. *J. Am. Chem. Soc.* **1967**, 89, 5661–5664.
14. Sørbotten, A.; Horn, S. J.; Eijsink, V. G. H.; Vårum, K. M. *FEBS J.* **2005**, 272, 538–549.